Nonuniform Chaotic Dynamics and Effects of Noise in Biochemical Systems

H. Herzel, W. Ebeling
Department of Physics, Humboldt-University Berlin, GDR

Th. Schulmeister
Central Institute of Molecular Biology, Academy of Sciences of the GDR, Berlin-Buch

Z. Naturforsch. **42 a**, 136–142 (1987); received August 8, 1986

Biochemical models capable of sustained oscillations and deterministic chaos are investigated. Chaos is characterized by exponential separation of near-by trajectories in the long-term average. However, we observed rather large deviations from purely exponential separation termed "nonuniformity". A quantitative description and consequences of nonuniformity are discussed.

Furthermore, the influence of short-correlated noise is treated using next-amplitude maps and Lyapunov exponents. Drastic amplification of fluctuations in non-chaotic systems and relative robustness of chaos were found.

1. Introduction

As a result of enzyme regulation in biochemical systems, a variety of dynamical patterns were found to occur [1–4]. Such a temporal selforganization is part of the biological regulation and might also prove responsible for failures in biological systems [5, 6].

In the following, Selkov-type systems are treated which may serve as qualitative models of metabolic pathways [7–10]. In these models sustained oscillations, coexistence of different attractors (e.g. birhythmicity in the sense of [3]), period-doubling, and deterministic chaos [9, 10] were found. In this paper we use specific models to discuss two problems which are of general interest: nonuniform dynamics and the effects of noise.

In Sect. 2 we introduce the models of consideration and apply usual techniques (phase portraits, next-amplitude maps, Lyapunov exponents). Chaotic behaviour is characterized by a positive Lyapunov exponent indicating that small perturbations grow exponentially in the long-term average. However, as we will show in Sect. 3 large deviations from this average growth occur, referred to as nonuniformity. Quantities are defined which measure the degree of this nonuniformity on different time scales.

It is widely recognized that biochemical systems are inherently noisy since they are open to their surroundings [11–14]. Thus it seems useful to study the effects of random fluctuations. In Sect. 4 mechanisms are discussed which may cause a drastic amplification of otherwise imperceptible fluctuations. The influence of noise on chaos is studied by the aid of next-amplitude maps and Lyapunov exponents in Section 5. Robustness of chaos and transitions from periodic to appearently chaotic behaviour are found.

Reprint requests to Dr. H. Herzel, Department of Physics, Humboldt-University, Invalidenstr. 42, DDR-1040 Berlin.

2. The Models

Our first system is a generalization of the well-known Selkov-oscillator describing glycolytic oscillations [7, 8]:

$$\mathrm{d}x/\mathrm{d}t = 1 - Bx - xy^2, \quad \mathrm{d}y/\mathrm{d}t = A(xy^2 - y). \qquad (1)$$

Here nonlinearity is due to an autocatalytic reaction of substrate x into product y. A detailed bifurcation diagram can be found elsewhere [8]. The main features of the dynamics are visualized in Fig. 1, where a stable limit cycle, a stable steady state on the x-axis and a separatrix between them can be seen. Despite the simplicity of (1) a Hopf-bifurcation and coexistence of attractors appear and, therefore, remarkable responses to fluctuations can be observed (see Section 4).

Deterministic chaos was found in an extended model containing in addition to (1) a reversible

0340-4811 / 87 / 0200-0136 $ 01.30/0. – Please order a reprint rather than making your own copy.

deposition of x into a inactive form z [9]:

$$\mathrm{d}x/\mathrm{d}t = 1 - Bx - xy^2 - Exy + z,$$

$$\mathrm{d}y/\mathrm{d}t = A(xy^2 - y + D), \quad \mathrm{d}z/\mathrm{d}t = F(Exy - z). \quad (2)$$

A bifurcation diagram and some routes to chaos are discussed in [9]. In the following only E will be varied and the other parameters are kept constant ($A = 4$; $B = 0.35$; $D = 0.1$; $F = 0.2$).

In 1978 the nonperiodic long-term behaviour of solutions of (2) was taken as an indicator of chaos [9]. Today, Lyapunov exponents describing the stability properties of trajectories are widely used as quantitative measurements of chaos [15, 16]. They describe the averaged stability properties of a trajectory on an attractor. For computation of Lyapunov exponents the linearized equations have to be solved:

$$\mathrm{d}\boldsymbol{q}/\mathrm{d}t = J(\boldsymbol{x})\,\boldsymbol{q} \quad (3)$$

($J(\boldsymbol{x})$ = Jacobimatrix, $\boldsymbol{x} \equiv (x, y, z)$).

These equations govern the behaviour of infinitesimal deviations $\boldsymbol{q}(t)$ from a trajectory $\boldsymbol{x}(t)$. The growth of the Euclidean norm of $\boldsymbol{q}$ leads for almost all initial vectors $\boldsymbol{q}(0)$ to the maximum Lyapunov exponent λ_1 [15]:

$$\lambda_1 = \lim_{t\to\infty} \left\{ \frac{1}{t} \ln \frac{\| \boldsymbol{q}(t) \|}{\| \boldsymbol{q}(0) \|} \right\}. \quad (4)$$

The sum of all Lyapunov exponents related to the contraction of phase space volume is given by the mean divergence:

$$\lambda_1 + \lambda_2 + \lambda_3 \quad (5)$$

$$= \lim_{t\to\infty} \frac{1}{t} \int_0^t (-B - y^2 - Ey + 2Axy - A - F)\,\mathrm{d}t'.$$

Since one Lyapunov exponent vanishes [15], we can compute the whole Lyapunov spectrum from (2)–(5). In this way the following estimations were obtained for a representative parameter value $E = 1.5$ (integration time: 50000):

$$\lambda_1 = 0.0285 \pm 0.0005,$$

$$\lambda_2 = 0,$$

$$\lambda_3 = -0.248 \pm 0.001. \quad (6)$$

Figure 2 shows how the maximum Lyapunov exponent λ_1 depends on parameter E. So-called periodic windows ($\lambda_1 = 0$) are interspersed among chaotic

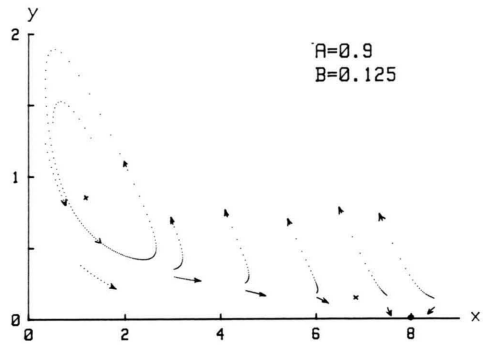

Fig. 1. Representative stroboscopic phase protrait to (1) with a stable node (●), unstable stationary points (×) and a stable limit cycle. Every 0.1 time units a point was plotted and thus fast and slow "motion" can be distinguished.

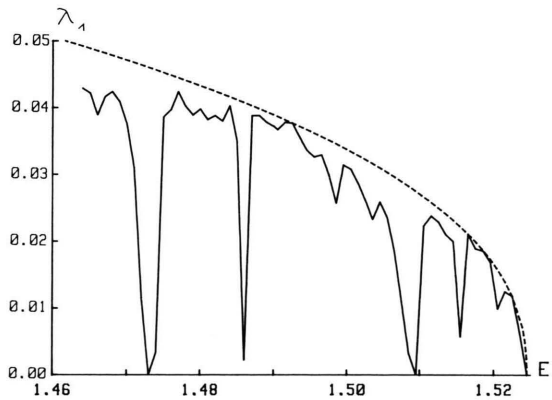

Fig. 2. Maximum Lyapunov exponent λ_1 near the onset of chaos (step width $\Delta E = 0.001$, integration times: 6000). Neighboring points have been joined by a straight line to guide the eye. The envelope (see (7)) is depicted as a dashed line.

parameters ($\lambda_1 > 0$). The onset of chaos around $E_c = 1.5245$ is characterized by the "period-doubling scenario" [9]. Therefore, one may expect a universal envelope of $\lambda_1(E)$ [17]:

$$\lambda_1(E) \sim |E - E_c|^{\beta}, \quad (\beta = 0.4498\ldots). \quad (7)$$

Such a power law indeed was found in our system (dashed line in Fig. 2) with an exponent $\beta = 0.42 \pm 0.04$. Thus, once more an astonishing universality near the onset of chaos is indicated.

Now we describe the solutions of (2) in the phase space spanned by the concentration variables. After a transient time trajectories are captured by the attractor. Periodic motion corresponds to an attracting limit cycle (see e.g. Fig. 1) whereas chaotic

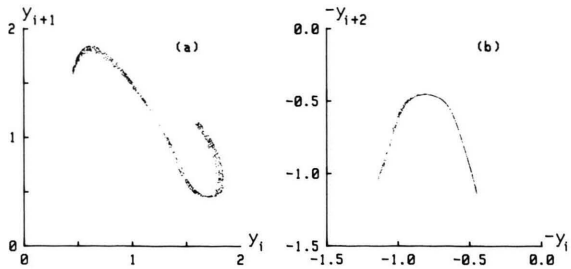

Fig. 3. Next-amplitude maps of chaos in (2) ($E = 1.5$). (a) Maximum of $y(t)$ versus the preceding one. (b) Maximum of $y(t)$ versus the maximum two oscillations before.

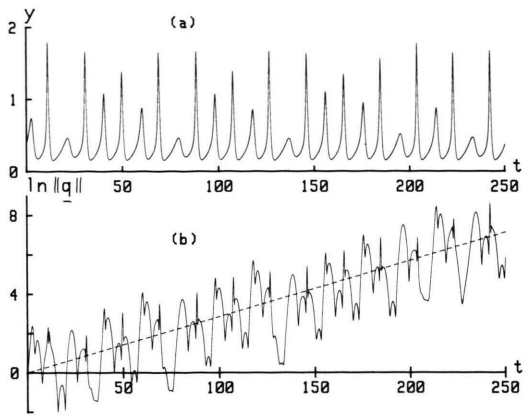

Fig. 4. (a) Chaotic oscillations of the concentration $y(t)$ (Eqs. (2); $E = 1.5$). (b) Corresponding growth of a perturbation $\boldsymbol{q}$ using (3) ($\| \boldsymbol{q}(0) \| = 1$). Note the deviations from the average behaviour (dashed line).

motion takes place on "strange attractors" which can be characterized by non-integer dimensions [18].

The Kaplan-Yorke dimension [19] follows from the Lyapunov exponents in (6):

$$D_{\mathrm{KY}} = 2 + \frac{\lambda_1}{|\lambda_3|} = 2.115 \pm 0.003 . \tag{8}$$

Since this value is slightly above two, the attractor is somewhat similar to a two-dimensional surface and, therefore, Poincaré sections or next-amplitude maps resemble one-dimensional curves. The next-amplitude maps in Fig. 3 are obtained from sequences of maximum y-values which are stored during the integration of (2). Since Fig. 3a reveals a two-band structure, it appears desirable to use every second maximum only. Thus the curve in Fig. 3b is derived. The similarity with the logistic map is not surprising because period-doubling was observed at adjacent parameters [9].

So far we have obtained some insight into the chaotic properties by using standard techniques (Lyapunov exponents, next-amplitude maps).

In the next section it will be demonstrated that the exponential separation of near-by trajectories must be understood as average behaviour. Deviations from the exponential growth turn out to be rather important, at least in chemical systems.

3. Nonuniform Dynamics

In order to produce temporal self-organization in chemical systems, several reactions are necessary. The reaction rates can vary widely and, therefore, the dynamics of chemical systems is usually very nonuniform. This means that the phase space velocities and the stability properties of trajectories fluctuate strongly.

It was shown in the preceding section that the norm of an infinitesimal perturbation grows exponentially in the long-term average (see (4)). However, the realization in Fig. 4 visualizes drastic deviations from average behaviour (dashed line). To quantify this nonuniformity, we return to (2)–(3) and discuss the growth of the Euclidean norm $\| \boldsymbol{q}(t) \|$ in some more detail:

$$\frac{\mathrm{d}}{\mathrm{d}t} \| \boldsymbol{q} \| = \frac{\sum_{i,j} J_{ij}(\boldsymbol{x})\, q_i\, q_j}{\sum_i q_i^2} \| \boldsymbol{q} \| \equiv L(\boldsymbol{x}, \boldsymbol{q}) \| \boldsymbol{q} \| . \tag{9}$$

Thus a time dependent divergence rate $L(\boldsymbol{x}, q)$ is derived which depends on the trajectory $\boldsymbol{x}$ and the direction of $\boldsymbol{q}$. With increasing time transients die out and almost all perturbations $\boldsymbol{q}$ are oriented into the direction of maximum expansion [15] and, therefore, the statistical properties of $L(\boldsymbol{x}, q)$ are assumed to be independent of the initial conditions. Equation (4) implies that the long-term average of $L(\boldsymbol{x}, q)$ equals λ_1. Now we define the following growth rates:

$$l_i(\tau) = \int_{t_i}^{t_i+\tau} L(\boldsymbol{x}, \boldsymbol{q})\, \mathrm{d}t = \ln \frac{\| \boldsymbol{q}(t_i + \tau) \|}{\| \boldsymbol{q}(t_i) \|} . \tag{10}$$

The quantities $l_i(\tau)$ measure the exponential change of the length of $\boldsymbol{q}(t)$ during the time interval τ when the system is moving along the trajectory from $\boldsymbol{x}(t_i)$

to $\boldsymbol{x}(t_i + \tau)$. Thus, the deviation from average behaviour can be measured on arbitrary time scales by the ratio of the standard deviation $\Delta l(\tau)$ to the mean value $\langle l(\tau)\rangle$ (averaging over ensembles $l_i(\tau)$ corresponds to time averages).

$$\Delta l(\tau) = (\langle l^2(\tau)\rangle - \langle l(\tau)\rangle^2)^{1/2}, \quad \langle l(\tau)\rangle = \lambda_1 \tau. \tag{11}$$

For small or large time scales τ, previously defined quantities can be recovered: the "Non-Uniformity Factor" (NUF) [20, 21] and a "diffusion constant" D [18, 22].

$$\text{NUF} \equiv \lambda_1 \cdot \lim_{\tau \to 0} \frac{\Delta(\tau)}{\langle l(\tau)\rangle},$$

$$D \equiv \frac{1}{2} \cdot \lim_{\tau \to \infty} \frac{(\Delta l(\tau))^2}{\tau}. \tag{12}$$

Table 1 contains information about the nonuniformity in our model on different time scales.

It can be concluded that only on large time scales ($\tau \gg 100$) the growth of perturbations $\boldsymbol{q}$ is actually governed by the maximum Lyapunov exponent. On time scales of only few oscillations (mean "period" $\langle T\rangle \approx 9.6$), expansion as well as contraction of perturbations can be found. These statements are in good accordance with the actual growth of the realization in Fig. 4. The concept of nonuniformity on arbitrary time scales was applied to one-dimensional maps in [23]. There it turns out again that a chemical system (Belousov-Zhabotinsky map) is characterized by strong nonuniformity. Our assumption of nonuniformity being a typical property of chemical chaos will be studied in more detail in a forthcoming paper.

Nonuniform dynamics is intimately related to the computational effort which is necessary to estimate Lyapunov exponents. Beyond this, the important question of state predictability depends on the degree of nonuniformity [24].

Table 1. Measures of nonuniformity (see (11)) on different time scales ($E = 1.5$, integration time: 10^4).

τ	$\Delta l(\tau)$	$\frac{\Delta l(\tau)}{\langle l(\tau)\rangle}$
0.1	0.128 ± 0.002	46 ± 2
0.2	0.247 ± 0.002	44 ± 2
1	0.88 ± 0.002	31 ± 2
10	1.96 ± 0.1	7 ± 0.5
100	2.14 ± 0.5	0.75 ± 0.2

From [18] it follows that nonuniform dynamics is closely connected with a complicated structure of attractors. Such an inhomogeneity of attractors can be treated by the concept of generalized attractor dimensions. Particularly, the differences between probabilistic dimensions measure the degree of inhomogeneity [18]. It was shown in [25] that our attractor ($E = 1.5$) is indeed a very "inhomogenous fractal" since the correlation exponent [18] $D_2 = 2.02 \pm 0.06$ differs considerably from the Kaplan-Yorke dimension (see (8)).

Thus we emphasize that chemical systems typically exhibit nonuniformity and inhomogeneous attractors and, therefore, a proper description should include a treatment of these properties.

4. Amplification of Noise in Non-Chaotic Systems

Real macroscopic systems are always in contact with sources of fluctuations. Besides thermal noise, a fluctuating input, the discrete number of reacting particles and "hidden" reactions are possible sources of random perturbations.

Here the wide class of additive short-correlated noise is simulated by adding every 0.1 time units uncorrelated Gaussian pseudo-random numbers (standard deviation Q) to the solutions of (1) or (2). In this way, realizations (Figs. 5 and 6) and next-amplitude maps (Figs. 9 and 10) were obtained. Furthermore, the maximum Lyapunov exponent λ_1 is computed in the presence of fluctuations. For this purpose in (3) the deterministic trajectory $\boldsymbol{x}$ was replaced by the perturbed orbit [26]. By this procedure λ_1 is defined via linearization along noisy trajectories, and thus it describes the separation of near-by orbits subject to the same external noise

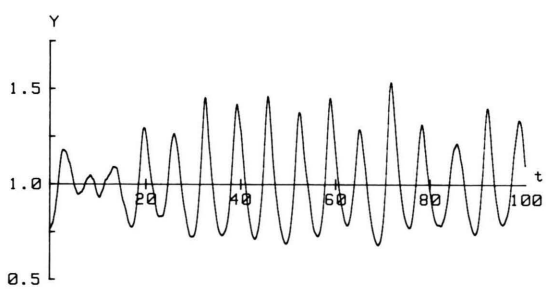

Fig. 5. Noise-induced oscillations near the Hopf bifurcation (Eqs. (1); $A = 0.95$; $B = 0$). The fluctuations act on $x(t)$ with $Q = 0.02$.

field. If near-by trajectories are influenced by different realization of random noise the situation is much more complicated. Then we can expect in addition to an exponential separation described by $\lambda_1 > 0$ a power-law separation due to noise which is well-known from diffusion [27].

First of all some effects of noise on two-dimensional systems are discussed. Under certain circumstances drastic amplification of fluctuations appears which can easily be confused with truly chaotic behaviour. Thus, our examples contain some warning in the present chaos euphoria to identify any large nonperiodic oscillations as deterministic chaos.

As a first example the Selkov-oscillator of (1) is treated at the parameters given in Figure 5. These values correspond to a weakly damped focus $(x, y) = (1, 1)$, i.e. deterministic trajectories approach this steady state with damped oscillations. The realization in Fig. 5 shows relatively regular noise-induced oscillations with amplitudes drastically exceeding the noise level ($Q = 0.02$).

Now we focus our attention to another kind of irregular oscillations due to fluctuations as demonstrated in Figure 6. At these parameter-values each deterministic trajectory approaches the stable node $(x, y) = (1/B, 0)$ (see Figure 1). On the contrary, stochastic realizations may cross the separatrix located slightly above the x-axis and return to the node after a high burst [28]. In both cases, the stochastic origin of the oscillations can be detected by negative Lyapunov exponents:

$$\begin{aligned} &\text{Fig. 5:} \quad \lambda_1 = -0.035 \pm 0.002, \\ &\text{Fig. 6:} \quad \lambda_1 = -0.15 \pm 0.02. \end{aligned} \tag{13}$$

However, we found another system with noise-induced instability, i.e. with $\lambda_1 > 0$ due to fluctuations:

$$\frac{\mathrm{d}x^2}{\mathrm{d}t^2} + 0.2 \cdot \frac{\mathrm{d}x}{\mathrm{d}t} - 10x + 100x^3 = \eta(t). \tag{14}$$

This double-well oscillator was studied intensively under periodic excitation [29]. Influenced by a random force $\eta(t)$ (every 0.05 time units Gaussian random numbers with variance 0.005 were added) similar oscillations as in the chaotic case [29] occur (see Figure 7a). This noise amplifier can be interpreted as a combination of the previously discussed cases, since it contains weakly damped focuses and

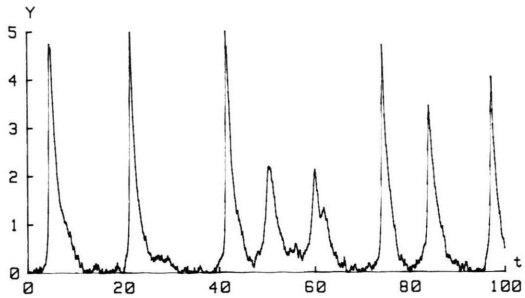

Fig. 6. Burst oscillations due to crossing of a separatrix (Eqs. (1), $A = 1.0$, $B = 0.125$). Noise acts on $x(t)$, $y(t)$ with $Q = 0.05$.

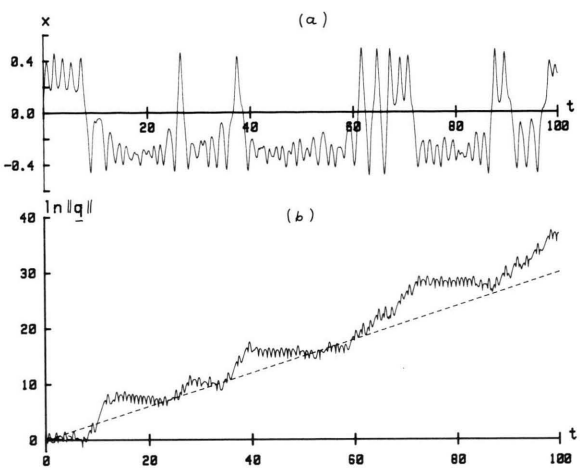

Fig. 7. (a) Noise-induced oscillation of the double-well oscillator (Eq. (14)). (b) Corresponding growth of a perturbation $\boldsymbol{q}$ using (3). Note the exponential growth in the average (dashed line) and the sudden increase of $\|\boldsymbol{q}\|$ due to noise-induced jumps to the other focus.

a separatrix. The unexpected result

$$\lambda_1 = 0.3 \pm 0.04 \tag{15}$$

can be understood from Figure 7b. As in Fig. 4, the behaviour of a perturbation $\boldsymbol{q}$ is shown, and in this way the origin of the instability can be detected. Noise may kick the system from positive to negative x-values (and vice versa) and thus the strong instability around $x = 0$ is responsible for the overall instability expressed by (15).

The chosen examples illustrate that fluctuations can be amplified to macroscopic proportions and thus easily be mistaken for deterministic chaos. However, powerful new methods of time series analysis are developed which allow chaos to be distinguished from stochastic oscillations [16, 30].

Besides our examples, further references [2, 31, 32] suggest that the amplification of noise due to local instability, marginal stability near bifurcations and coexistence of attractors might be of similar importance as chaos itself.

5. The Influence of Noise Chaotic on Dynamics

In order to cross the interface between mathematical models [1–3, 9] and experimental evidence of chaos [33, 34], it is appropriate to incorporate the effects of fluctuations [17, 35]. Therefore, we consider (2) with nonvanishing noise, i.e. we add random perturbations to the solutions $x(t)$ and $y(t)$ (standard deviation Q). In the presence of noise the same properties and techniques as in Sect. 2 are chosen: the instability of orbits, measured by Lyapunov exponents, and the structure of attractors, displayed by next-amplitude maps.

The full line in Fig. 8 shows the maximum Lyapunov exponent λ_1 versus the parameter E in the absence of noise, whereas the dashed line visualizes the smoothing effect of noise. Particularly, it turns out that the thresholds of chaos are shifted and that windows disappear.

One may expect that chaos responds very sensitively to fluctuations as trajectories are unstable, but averaged properties such as the Lyapunov exponent λ_1 are relatively robust. Moreover, the parameter region of positive λ_1 is enlarged by noise.

In the following we want to study the effects of fluctuations with the aid of next-amplitude maps. A comparison of Fig. 3a with Fig. 9 reveals that the two bands merge due to noise, whereas the general structure is preserved.

Now the "window" at $E = 1.5095$ (compare Fig. 2) is considered. Figure 10 shows that the 6-period cycle is destroyed by the noise and that the behaviour reminds to chaos at adjacent parameters (see Figure 3). An explanation of the seemingly chaotic behaviour in Fig. 10 is connected with chaotic transient [36]: Deterministically after some transient time on a chaotic repeller the trajectories ultimately fall onto the periodic attractor. Since these transients are more robust against fluctuations, the noisy trajectories resemble nearby (in parameter space) chaotic orbits. Summarizing, we conclude that in agreement with other studies [13, 17, 35] essential properties of chaos persist in the presence

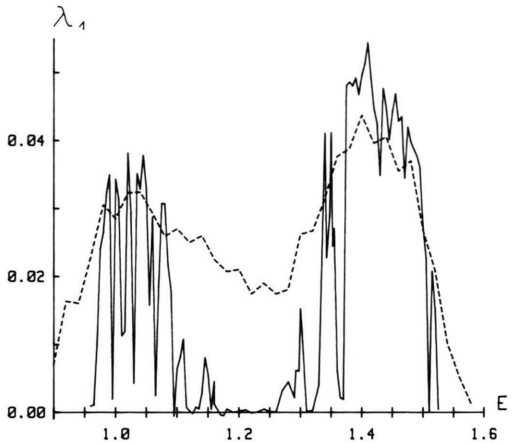

Fig. 8. Maximum Lyapunov exponent versus the parameter E. Neighboring points have been joined by lines to guide the eye. Integration times: 6000; full line: deterministic case ($Q = 0$); $\Delta E = 0.005$; dashed line: noisy case ($Q = 0.0005$); $\Delta E = 0.02$.

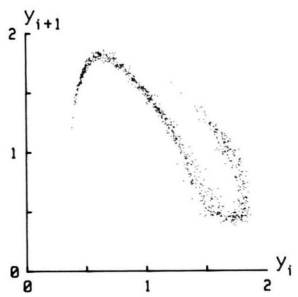

Fig. 9. Next-amplitude map as in Fig. 3a but nonvanishing noise ($Q = 0.0002$).

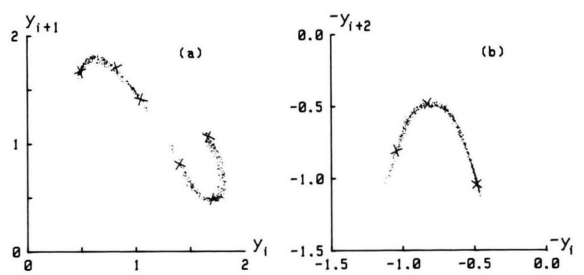

Fig. 10. Next-amplitude maps at $E = 1.5095$ (deterministically a window) in the presence of fluctuations ($Q = 0.0004$). The deterministic cycle is visualized by crosses. (a) Maximum of $y(t)$ versus the preceding one; (b) maximum of $y(t)$ versus the maximum two oscillations before.

of noise. Thus chaos is observable in experiments and numerical errors have no dramatic consequences.

6. Concluding Remarks

Deterministic chaos appears in rather simple biochemical models. However, the corresponding parameter regions in autonomous systems seem to be small [3, 9]. On the contrary, it was quite easy to find chaos via periodic modulation of the parameters in (1) [10].

Chaos appearing in (2) was measured by Lyapunov exponents and the Kaplan-Yorke dimension. It turns out, however, that these averaged quantities only partially describe what actually is going on, since nonuniform dynamics and inhomogeneous attractors are characteristic properties of chemical chaos. The exponential instability is, therefore, essential on large time scales only.

It is worth mentioning that the concept of nonuniformity seems to be related to the problem of weather forecast. Lorenz investigated the error growth of atmospheric predictions [37] and found some indications of exponential instability on time scales of about ten days whereas the error growth over a few days is characterized by large deviations from average behaviour.

In Sect. 5 the interaction between two kinds of stochasticity, deterministic chaos and short-correlated noise, was studied. Whereas individual trajectories respond sensitively to perturbations, overall properties such as Lyapunov exponents and the structure of next-amplitude maps turn out to be robust.

In certain systems, however, effects of noise were found which lead to decreasing Lyapunov exponents [26, 38, 39]. These effects are the subject of a forthcoming paper.

Finally we want to emphasize that the studies of biochemical chaos are still at their very beginning. Therefore, further experimental and theoretical investigations are desirable, and we propose that measuring nonuniformity as well as effects of fluctuations should be included.

[1] O. E. Rössler, Z. Naturforsch. **31 a,** 258 (1976).
[2] B. Hess and M. Markus, Ber. Bunsenges. Phys. Chem. **89,** 642 (1985).
[3] O. Decroly and A. Goldbeter, Proc. Natl. Acad. Sci. USA **79,** 6917 (1982).
[4] W. Ebeling and R. Feistel, Physik der Selbstorgnisation und Evolution, Akademie-Verlag, Berlin 1982.
[5] A. V. Holden (ed.), Chaos, Manchester University Press, Manchester 1986.
[6] M. C. Mackey and L. Glass, Science **197,** 287 (1977).
[7] E. E. Selkov, Eur. J. Bioch. **4,** 79 (1968).
[8] Th. Schulmeister and E. E. Selkov, stud. biophys. **65,** 121 (1977).
[9] Th. Schulmeister, stud. biophys. **72,** 205 (1978).
[10] Th. Schulmeister and H. Herzel, ZAMM, to appear.
[11] B. Hess and A. Boiteux, Ber. Bunsenges. Phys. Chem. **84,** 346 (1980).
[12] H. Herzel, Thesis, Humboldt-University, Berlin 1985.
[13] L. F. Olsen, Z. Naturforsch. **40 a,** 1283 (1985).
[14] H. Herzel and Th. Schulmeister, in: Proc. Dynamical Systems and Environmental Models (W. Ebeling and M. Peschel, eds.), Akademie-Verlag, Berlin 1986.
[15] J. P. Eckmann and D. Ruelle, Rev. Mod. Phys. **57,** 617 (1985).
[16] A. Wolf, J. B. Swift, H. L. Swinney, and J. A. Vastano, Physica **16 D,** 285 (1985).
[17] J. P. Crutchfield, J. D. Farmer, and B. A. Hubermann, Phys. Reports **92,** 45 (1982).
[18] P. Grassberger and I. Procaccia, Physica **13 D,** 34 (1984).
[19] J. L. Kaplan and J. A. Yorke, in: Lecture Notes in Math., vol. 730 (H. O. Peitgen and H. O. Walter, eds.), Springer-Verlag, Berlin 1978.
[20] J. S. Nicolis, G. Mayer-Kress, and G. Haubs, Z. Naturforsch. **38 a,** 1157 (1983).
[21] G. Haubs and H. Haken, Z. Phys. B **59,** 459 (1985).
[22] H. Fujisaka, Progr. Theor. Phys. **71,** 513 (1984).
[23] H. Herzel and B. Pompe, Phys. Lett. A, submitted.
[24] B. Pompe, J. Kruscha, and R. W. Leven, Z. Naturforsch., to appear.
[25] H. Herzel and Th. Schulmeister, Syst. Anal. Mod. Sim., to appear.
[26] L. Arnold, preprint Nr. 61, Universität Bremen 1982.
[27] S. Grossmann and I. Procaccia, Phys. Rev. A **29,** 1358 (1984).
[28] H. Engel-Herbert, W. Ebeling, and H. Herzel, in: Temporal Order (L. Rensing and N. I. Jaeger, eds.). Springer-Verlag, Berlin 1985.
[29] P. Holmes, Phil. Roy. A **292,** 419 (1979).
[30] J. Kurths and H. Herzel, Physica D, to appear.
[31] J. D. Farmer, preprint, Los Alamos 1984.
[32] M. Iansiti, Quing Hu, R. M. Westervelt, and M. Tinkham, Phys. Rev. Lett. **55,** 746 (1985).
[33] L. F. Olsen and H. Degn, Nature London **267,** 177 (1977).
[34] A. Arneodo, F. Argoul, P. Richetti, and J. C. Roux, preprint, Bordeaux 1985.
[35] W. M. Schaffer, S. Ellner, and M. Kot, J. Math. Biol., in press.
[36] H. Kantz and P. Grassberger, Physica **17 D,** 75 (1985).
[37] E. N. Lorenz, Tellus **34,** 505 (1982).
[38] M. Matsumoto and I. Tsuda, J. Stat. Phys. **31,** 87 (1983).
[39] H. Herzel and W. Ebeling, Phys. Lett. **111 A,** 1 (1985).